Reference *Biol. Bull.* 198: 272–283 (April 2000)

Vacuolar-type ATPase in the Accessory Boring Organ of *Nucella lamellosa* (Gmelin) (Mollusca: Gastropoda): Role in Shell Penetration

ERIC S. CLELLAND AND A. S. M. SALEUDDIN*

Department of Biology, York University, Toronto, Ontario, Canada M3J 1P3

Abstract. The structure and function of the accessory boring organ (ABO) of muricid gastropods has been described in numerous studies, and the ABO of *Nucella lamellosa* was found to be similar to those of other muricid species. The active cap region of the ABO is composed of tall, mitochondria-rich cells with distinct brush borders at their apicies, surrounding a hemolymph-containing central sinus. Using antibodies specific for vacuolar-type ATPase (V-ATPase), enzyme immunoreactivity was found to be limited to the brush border of the epithelial cells. Electron immunohistochemistry revealed that V-ATPase immunoreactivity resides in the plasma membranes of the microvilli. Immunodot blotting using yeast V-ATPase as a positive control confirmed the specificity of the reactions. SDS-PAGE of membrane suspensions from the ABO revealed protein bands of the requisite molecular weight for V-ATPase subunits. Western blots suggest that antibodies raised against mammalian V-ATPase subunits recognize subunits of the molluscan V-ATPase. The molecular weights of these identified subunits are similar to those in mammals. The V-ATPase-specific inhibitor bafilomycin A_1 inhibited ATPase activity in samples of ABO homogenate by about 10% relative to control, providing further evidence for the presence of V-ATPase. Specific V-ATPase activity was about 67 picomoles of inorganic phosphate per microgram of protein per minute in the homogenate. Collectively this evidence strongly suggests that a vacuolar-type proton transporting ATPase is present in the brush border of the accessory boring organ of *Nucella lamellosa*, and is responsible for acidifying secretions from this gland. Similarities between the ABO, osteoclasts, and the mantle of freshwater bivalves also suggest that the mechanism for decalcification of calcareous substrates is conserved.

Received 14 October 1999; accepted 27 December 1999.

* To whom correspondence should be addressed. E-mail: saber@yorku.ca

Introduction

Nucella lamellosa is a predatory marine snail of the family Muricidae (=Muricacea); it is commonly found in intertidal and subtidal zones along the Pacific Northwest coast of North America, ranging from the Aleutian Islands to Santa Cruz, California (Collins *et al.*, 1996). Muricid gastropods such as whelks and oyster drills feed on a variety of invertebrates such as bivalves, barnacles, small crabs, polychaetes, and occasionally carrion (Fretter and Graham, 1962; Carriker, 1981; West, 1986, 1988). The snails use a chemomechanical process to bore through bivalve shells and other calcareous substrates. This process combines the secretion of acidic solution from the accessory boring organ (ABO), to soften the shell, with the rasping action of the radula, to remove the loosened material. Acidity as low as pH 3.8 (~4 pH units lower than the surrounding seawater) has been measured within bore holes created by drilling muricids (Carriker and Van Zandt, 1967). The ABO of muricids is located in the anterior region of the sole of the foot, and is everted by hydrostatic pressure of the hemolymph in actively drilling animals. The ABO consists of a cap (about 1–2.5 mm diameter) and stalk (about 0.4 mm in length); the cap is composed of a central sinus surrounded by a single layer of tall (200–300 μm), mitochondria-rich epithelial cells. These cells also possess prominent apical brush borders, are separated from the sinus by a thin, often indistinct basement membrane, and communicate with one another *via* gap junctions. The structure of the muricid ABO and the mechanism of shell boring by muricid (and naticid) gastropods have been reviewed by Carriker (1981).

Webb and Saleuddin (1977) postulated that acid ATPase

pumps residing in the apical membranes of the ABO epithelial cells are responsible for acidifying the secretions from the muricid ABO. Vacuolar-type ATPase (V-ATPase) proton pumps are now known to be present in all eukaryotic cells, where they energize endomembranes (Finbow and Harrison, 1997). V-ATPases have also been detected in the plasma membrane of specialized cells in many animal epithelial tissues such as frog skin (Ehrenfeld and Klein, 1997), gills of freshwater fish (Lin *et al.*, 1994) and crustaceans (Onken and Putzenlechner, 1995), and in insect Malpighian tubules (Al-Fifi *et al.*, 1998) and midguts (Schweikel *et al.*, 1989), where they are used to generate transmembrane potentials that power the transport of other ions (*e.g.*, Na^+, K^+, CO_3^-). In osteoclasts (Nordström *et al.*, 1997), kidney collecting-duct cells (Brown *et al.*, 1988), urinary bladders (Lubansky and Arruda, 1985), epididymis (Brown *et al.*, 1997), salivary glands (Just and Walz, 1994), and the mantle of freshwater bivalves (Hudson, 1993; da Costa *et al.*, 1999), V-ATPases serve to acidify the extracellular environment by extruding protons from the cytoplasm of epithelial cells. Comprehensive reviews of V-ATPases are found in Brown and Breton (1996); Finbow and Harrison (1997); Harvey *et al.* (1998); Nelson and Harvey (1999); Wieczorek *et al.* (1999). Cells that possess plasma membrane V-ATPase pumps have common characteristics that closely resemble those of the epithelial cells of the muricid ABO. Furthermore, models describing V-ATPase-driven proton transport in various animal tissues (see Harvey *et al.*, 1998) are similar to the Webb and Saleuddin (1977) model describing proton transport in muricid ABOs; however, V-ATPases were unknown at the time of this earlier publication.

In this study we investigated a muricid ABO to determine whether V-ATPase pumps are present. Taking advantage of the conserved structure of V-ATPase molecules (Nelson and Harvey, 1999) and the cross reactivity (across phyla) of antibodies raised against V-ATPase subunits (Russell *et al.*, 1992), we probed sections of ABO tissue using primary antibodies directed against the A (~70 kDa), B (~60 kDa), and d (~39 kDa) subunits of the V-ATPase enzyme. Immunoblotting studies on extracts of ABOs were also completed. Additionally, the specific V-ATPase inhibitor bafilomycin A_1 (Bowman *et al.*, 1988) was used in assays of ATPase activity in ABO extracts to reveal the contribution of V-ATPase to the overall ATPase activity.

Materials and Methods

Animals

Specimens of *Nucella lamellosa* were obtained from Westwind Sealab Supplies, Victoria, British Columbia, at various times throughout the year. The animals were maintained in 50-l aquaria in artificial seawater (ASW; Instant Ocean from Aquarium Systems, Mentor, Ohio), pH 7.2–8.0; 950–1000 mmol/kg H_2O, at 5°C under a 12L:12D photoperiod. Live blue mussels were provided as the major food source. Under these conditions, the snails appeared to thrive, feeding regularly and depositing egg sacs on the walls of the aquaria.

Experimental animals ranging in length from 2 to 5 cm were chosen at random and narcotized in ASW diluted with an equal volume of 20% $MgSO_4 \cdot 7H_2O$ (Pantin, 1964). The shells were cracked using a bench vise, and the soft body was removed and rinsed clean of shell fragments. In accordance with the procedure of Carriker *et al.* (1963), the animals were cut in two at the base of the visceral hump, separating the viscera from the pedal mass. The pedal mass was pinned in a paraffin-based dissecting dish, with the ventral sole of the foot spread uppermost so as to expose the crypt of the retracted boring organ. Gentle pressure was applied to evert the ABO. The ABO, along with a short portion of the stalk, was excised using iridectomy scissors and fine forceps.

Accessory boring organs for microscopic examination were transferred to the appropriate fixative, while those to be used for biochemical assay, immunoblotting, or gel electrophoresis were transferred to homogenization buffer for immediate processing or were frozen in liquid nitrogen and stored at −80°C until required.

Chemicals and Antibodies

Unless otherwise specified, all chemicals were reagent grade, and were obtained from Sigma-Aldrich Canada Ltd.

Affinity-purified polyclonal antibodies raised against bovine V-ATPase d (39 kDa) and B (~60 kDa) subunits (raised in rabbit) and monoclonal antibodies raised against yeast (*Saccharomyces cerevisiae*) V-ATPase B (~60 kDa) and A (~70 kDa) subunits were donated by Dr. Sergio Grinstein and Dr. Morris Manolson of the University of Toronto. A sample of yeast V-ATPase was also supplied by Dr. Manolson.

Light microscopy

Accessory boring organs were excised from *Nucella* and fixed in Hollande Bouin's fixative for 12–18 h. The tissues were rinsed in distilled water, dehydrated, and embedded in paraffin. Serial sections of 8 μm thickness were deparaffinized, rehydrated, and stained in Mallory-Heidenhain for 5 min (Humason, 1967). Sections were viewed using a Leitz orthoplan microscope, and micrographs were taken using a Wild-Heerbrugg MPS 45/51S system.

Light microscope immunocytochemistry

Accessory boring organs were fixed and embedded as above. Serial sections were mounted on multiwell glass slides coated with 0.5% chrome alum and 0.5% gelatin. Sections to be used with alkaline-phosphatase-conjugated secondary antibodies were treated with 20% acetic acid for 30 min after rehydration; those probed with HRP (horse-

radish peroxidase)-conjugated secondary antibodies were treated with 0.3% H_2O_2 in methanol for 30 min prior to rehydration in graded ethanol. Secondary antibody conjugates (Sigma) were raised in goat and directed against either rabbit or mouse whole IgG. The antibodies were conjugated to either alkaline phosphatase or HRP. Tissues were rinsed in glass distilled water (ddH_2O), followed by two or three rinses in phosphate buffered saline (PBS). Nonspecific binding was blocked by incubation in PBS containing 5% normal goat serum (NGS) and 0.2% Triton X-100 (incubation buffer) for 1 h. Primary antibodies were applied undiluted from the stock provided (~20 μl was sufficient to cover each section), and sections were incubated for 12–18 h at 4°C. Control sections were maintained in incubation buffer without antibody. Following incubation, the primary antibodies were removed with several changes of incubation buffer over a period of 30 min. The sections were then incubated in secondary antibody conjugate (diluted 1:50 in incubation buffer) for 1 h at 22°C, then rinsed in PBS (three rinses, 5 min each) and finally in ddH_2O. Peroxidase was localized using Sigma Fast DAB Tablets (3,3′-diaminobenzidine tetrahydrochloride/H_2O_2), then sections were dehyrated and mounted as above. Alkaline phosphatase was localized using Sigma Fast BCIP/NBT tablets (5-bromo-4-chloro-3-indolyl-phosphate/nitro blue tetrazolium). The sections were mounted in aqueous media (5% polyvinyl alcohol; 30% glycerol), viewed, and photographed.

Transmission electron microscopy

Accessory boring organs were excised and fixed in a solution of 1% glutaraldehyde-0.1% paraformaldehyde in filtered ASW for 1 h at 22°C, then postfixed for 1 h in 1% aqueous osmium tetroxide at 0°C. Following fixation, the ABOs were rinsed in distilled water, dehydrated in graded ethanol, and embedded in epoxy resin. Thin sections (~80 nm thick) were cut using a diamond knife, floated onto Formvar-coated single-slot grids, and stained with uranyl acetate and lead citrate. Sections were viewed in a Philips EM201 transmission electron microscope.

Electron microscope immunocytochemistry

Accessory boring organs were excised from *Nucella*; rinsed in ASW; and fixed in 2% paraformaldehyde, 0.075 *M* lysine, 0.01 *M* sodium meta-periodate, in 0.037 *M* phosphate buffer, pH ~7.4 (PLP fixative; McClean and Nakane, 1974) for 2 h at 22°C. The tissues were thoroughly rinsed in distilled water, dehydrated to 70% ethanol, and embedded in LR-White resin (London Research Laboratories). The resin was polymerized under ultraviolet light for 96 h at 4°C. Thin sections were cut as described, collected on Formvar-coated 200 mesh nickel grids, and allowed to anneal overnight. The grids were first rinsed in distilled water and then in PBS, as for paraffin sections, and incubated in 5% NGS in PBS for 1 h to block nonspecific binding sites. Grids were floated on 25-μl droplets of primary antibody (anti-d subunit), and incubated in a humid chamber for 12 h at 22°C. The grids were rinsed three times in buffer (20 min each rinse) and incubated for 1 h in 10-nm gold-conjugated secondary antibody (BDH). Unbound secondary antibody was rinsed away with three changes (10 min each) of PBS and distilled water. The grids were stained with uranyl acetate and viewed as above.

Tissue preparation

Fresh or frozen ABOs (15 to 20) were homogenized on ice in 3 to 4 times their volume in buffer containing 20 m*M* Tris-HCl; 250 m*M* sucrose; 1 m*M* phenylmethyl sulfonyl fluoride (PMSF); 1 m*M* ethylene glycol bis (β-aminoethyl ether) *N, N, N′, N′*-tetraacetic acid (EGTA); 1 m*M* dithiothreitol (DTT); pH 7.4 (Rautiala *et al.*, 1993) using a motorized Teflon pestle in 1.5 ml polypropylene Eppendorf tubes. The homogenate was centrifuged at 1000 × *g* at 4°C for 15 min. The supernatant was collected, and the pellet was resuspended and recentrifuged. The resultant supernatant was combined with the first and used for ATPase assays without further purification, because more highly purified samples showed an apparent loss of activity.

For polyacrylamide gels and immunoblotting, the 1000 × *g* supernatant was subjected to further purification. It was centrifuged at 15,000 × *g* for 20 min, and the pellet discarded. The supernatant from this step was transferred to polyallomer centrifuge tubes, diluted with homogenization buffer to 500 μl, and centrifuged for 90 min at 100,000 × *g* using a Beckman Optima L-90K ultracentrifuge and SW65 rotor. The resultant supernatant was collected and the membrane pellet resuspended in 20–25 μl double distilled water (ddH_2O). Samples of the 15,000 × *g* and the 100,000 × *g* supernatants, as well as the membrane suspension, were frozen in liquid nitrogen and stored at −80°C until required.

Protein determination

Processed tissues were analyzed for their protein content using a Bio-Rad protein assay kit, which utilizes the method of Bradford (1976). Protein content was determined by comparison to a standard curve produced using bovine serum albumin (BSA).

Gel electrophoresis

SDS-PAGE was carried out using a Bio-Rad Mini-Protean II system. Samples diluted in buffer (50% H_2O; 0.0625% Tris-HCl, pH 6.8; 10% glycerol; 2% SDS; 5% 2-β mercaptoethanol; 0.0013% bromo-phenol blue) 1:4, were loaded onto 4%–15% (w/v) linear gradient SDS-PAGE precast gels (BioRad) or onto 9% (w/v) SDS-PAGE gels *via*

3.3% (w/v) stacking gels (Laemmli, 1970). The gels were run at 100 V for about 1 h, rinsed with ddH_2O, and stained for protein using Coomassie brilliant blue R-250 in fixative (40% methanol, 10% acetic acid). Nonspecific staining was removed in a solution of 40% methanol and 10% acetic acid. Gels were vacuum dried onto blotting paper and photographed.

Immunoblotting

For dot blots, samples of the 15,000 × *g* supernatant (3 μg or 15 μg total protein per sample) or purified yeast V-ATPase (1-μl and 2-μl samples) were pipetted onto methanol-activated PVDF membranes (0.45-μm pore size, Gelman Sciences) and allowed to air dry. The membranes were rinsed in Tris-buffered saline (TBS; 20 m*M* Tris-HCl, 500 m*M* NaCl, pH 7.5). Immunoblotting was carried out essentially according to Sheng and Schuster (1992). Experimental blots and positive control membranes were incubated with polyclonal antibodies (either anti-d or anti-B V-ATPase subunit) diluted 1:1000 in incubation buffer (TBS containing 0.5% BSA and 0.02% NaN_3) for 12 h at 4°C. Negative controls were kept in incubation buffer without primary antibody. The membranes were washed and probed using alkaline-phosphatase-conjugated anti-Ig G antibodies (diluted 1:4000 in incubation buffer) for 1 h at 22°C. After washing out the unbound secondary antibodies, the membranes were rinsed with several changes of ddH_2O, and staining was developed with Sigma Fast BCIP/NBT tablets. The membranes were allowed to air dry, and then photographed.

For Western blotting, 10-μg samples of the 100,000 × *g* resuspended pellet (diluted 1:4 in running buffer) and markers were loaded onto 9% SDS-PAGE gels and electrophoresed as described above. The gels were removed, rinsed in ddH_2O, then placed in transfer buffer (25 m*M* Tris, 192 m*M* glycine, 20% v/v methanol, pH 8.3) and equilibrated for 30 min with gentle agitation. PVDF membranes were wetted in 100% methanol and also allowed to equilibrate in transfer buffer. Blotting was completed using the Bio-Rad Mini Trans-Blot module for the Mini-Protean II system. Transfer was completed overnight at 4°C, after which the membranes were allowed to air dry, allowing the protein to adhere tightly to the PVDF membrane. Membranes were then placed in a solution of 0.3% H_2O_2 for 10 min to block endogenous peroxidase activity, rinsed in ddH_2O and TBS, then nonspecific binding sites were blocked as for the dot blots. Primary antibodies were applied as described for the dot blots and incubated overnight at 4°C. The membranes were washed in incubation buffer, incubated in 1% nonfat milk in TBS, and rinsed in incubation buffer. At this time the membranes were rinsed in TBS (3 times, 10 min each), and a "Histomark" Streptavidin-HRP system kit was employed (Kirkegaard and Perry Laboratories Inc. (KPL), Gaithersberg, Maryland). The membranes were incubated for 30 min at room temperature in 10% v/v NGS provided with the kit. The membranes were then transferred to the biotinylated antibody solution provided (diluted 1:4 in TBS) and incubated a further 30 min. The membranes were rinsed (3 times, 5 min each) in TBS containing 1% NGS, and incubated in streptavidin-peroxidase (diluted 1:4 from that provided) for an additional 30 min. Following this treatment, the membranes were rinsed in several changes of TBS, then in distilled water. Banding patterns were revealed using KPL TrueBlue peroxidase substrate. The membranes were allowed to dry, and were photographed.

ATPase assays

Ten to twenty-five microlitres of the homogenate (~15 μg protein per tube) were placed in 1.5-ml Eppendorf tubes, in 145 μl of assay buffer (2 m*M* $MgCl_2$, 20 m*M* KCl, 0.1 m*M* EGTA, 0.3 mg/ml BSA, 0.5 m*M* sodium azide (NaN_3) [to inhibit mitochondrial ATPase activity], 30 m*M* Tris-HCl, pH 7.5; modified from Al-Fifi *et al.*, 1998). To experimental samples, 5 μl of bafilomycin A_1 (Sigma) stock solution (10 μg diluted in 500 μl dimethylsulfoxide (DMSO)) was added, giving a final concentration of 1 μ*M* for the inhibitor. DMSO alone was added to the controls (Onken and Putzenlechner, 1995). Samples were incubated for 30 min at 22°C to allow the inhibitors to react. To initiate the ATPase reaction, 50 μl of 12 m*M* Mg^{2+}-ATP was added to the sample tubes (3 m*M* final concentration). The samples were reacted for 45 min at 37°C in a water bath, following which 400 μl of a 1:1 mixture of 1% polyoxyethylene 10 lauryl ether in distilled deionized water, and 1% ammonium molybdate in 0.9 *M* H_2SO_4 was added to stop the reaction (procedure modified from Atkinson *et al.*, 1973). The tubes were kept at room temperature for 10 min to allow the yellow color to develop. Absorbancy was then measured at 390 nm. The relative quantity of inorganic phosphate (Pi) was determined by comparison to a standard curve produced using phosphate standards as described by Atkinson *et al.* (1973). The total activity is expressed as the amount of Pi produced per microgram of total protein per minute. The V-ATPase activity was determined to be the difference between the amount of Pi produced by the controls in the absence of bafilomycin and the amount produced by experimental samples with bafilomycin.

Statistical analysis

Student's *t* tests were completed on the experimental ATPase assay data using GraphPad Instat v. 2.0 (GraphPad Software, San Diego, California).

Results

Structure of the Accessory Boring Organ

The structure of the ABO in *Nucella lamellosa* is shown in Figure 1, and is similar to that described for other

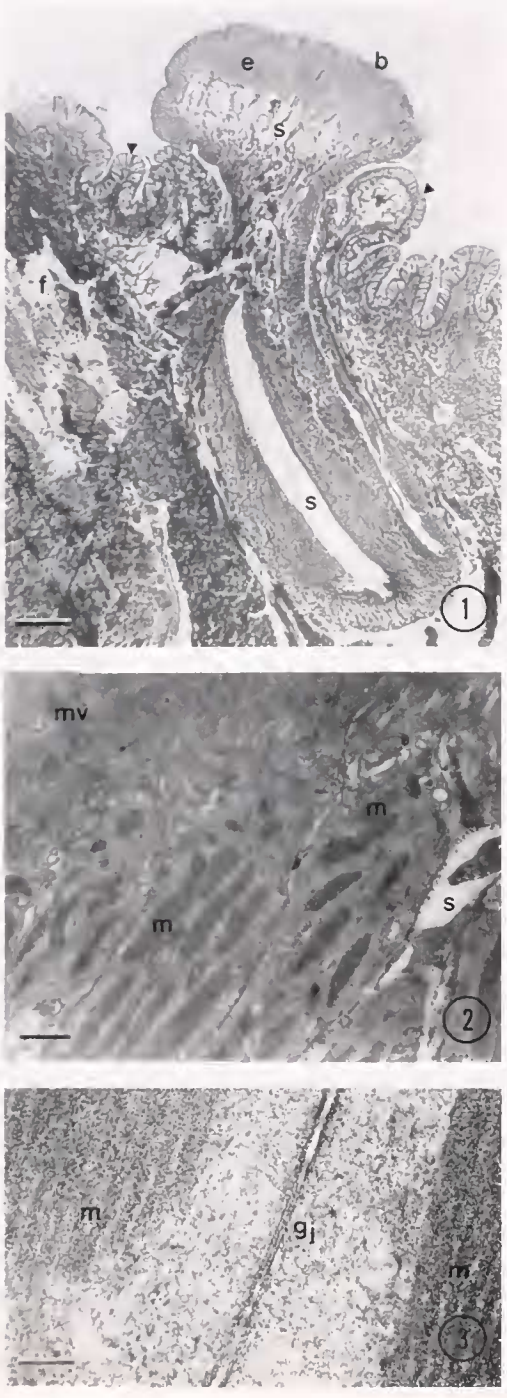

Figures 1–3. The accessory boring organ (ABO) of *Nucella lamellosa*.

Figure 1. Section of an everted ABO stained with Mallory-Heidenhain quick stain. Note the mushroom shape of the organ. The cap is comprised of a single layer of epithelial cells (e) surrounding a central sinus (s), which is continuous with the sinus in the stalk. The stalk invaginates into the foot (f). The epithelial cells of the ABO cap are long (200–300 μm), with a prominent brush border (b). By contrast, the epithelial cells of the surrounding foot tissue (arrow heads) are short (40 μm). Muscle is seen in the left lateral side of the stalk, and is presumably used to retract the ABO into its crypt (vestibule) in the foot. Scale bar: 200 μm.

muricids, in particular to that of *Thais (N.) lapillus* (Webb and Saleuddin, 1977). The cap of the ABO consists of a single layer of epithelial cells (e), surrounding a central sinus (s). The epithelial cells possess a distinct apical brush border (b). The stalk of the ABO invaginates into the foot (f), and also contains a sinus (s). The brush border of the epithelial cells is about 10–15 μm in height, and the cells themselves are tall (200–300 μm) and thin, with irregular basal infoldings abutting the central sinus. There is no distinct demarcation between the epithelial cells and the sinus. Interstitial spaces can be seen between the cells, providing additional surface area to the sinus. Nuclei are identifiable in the basal third of the cells, and other organelles occur distally to them. Strands of muscle and connective tissue can be observed spanning the sinus, loosely connecting the epithelium to the more muscularized stalk. The muscle in the stalk is probably involved in retracting the ABO into its vestibule within the foot.

By contrast, the surrounding foot epithelium (arrowheads) is composed of shorter columnar cells (~40 μm in height) without a brush border. An obvious basement membrane underlies these cells, separating them from the foot tissue below. The foot epithelium is composed mainly of goblet cells, which undoubtedly secrete mucus, serving to lubricate the foot and to seal it tightly to the substrate when the snail is drilling. At the electron microscope level, the apical area of the ABO epithelial cells (Fig. 2) shows the long microvilli (mv) that make up the brush border of the ABO, and the many mitochondria (m) within the cells. Dense granules are also present in the apical region of the cells. Gap junctions (gj) occurring between adjacent epithelial cells are commonly seen in the apical region (Fig. 3). These junctions are thought to facilitate communication between the cells, ensuring rapid and uniform response of the ABO epithelium (Webb and Saleuddin, 1977).

Immunocytochemical localization

Positive immunoreaction for V-ATPase was obtained using anti-d subunit primary antibody, with either alkaline phosphatase or HRP conjugates as secondary antibodies (Figs. 4, 5, 6). Immunoreaction was localized exclusively to the brush border region of the ABO. The surrounding foot epithelium (acting as built-in control for the sections) and other areas of the ABO showed no immunostaining. See-

Figure 2. Electron micrograph of the apical region of the ABO cap epithelium. Note the long microvilli (mv) of the brush border, the numerous mitochondria (m), and the interstitial spaces (s) between the cells. Dense granules seen in the cells may contain degradative enzymes. Scale bar: 1.5 μm.

Figure 3. Electron micrograph illustrating the presence of gap junctions (gj) between adjacent cells of the ABO cap. Also note the mitochondria (m). Scale bar: 100 nm.

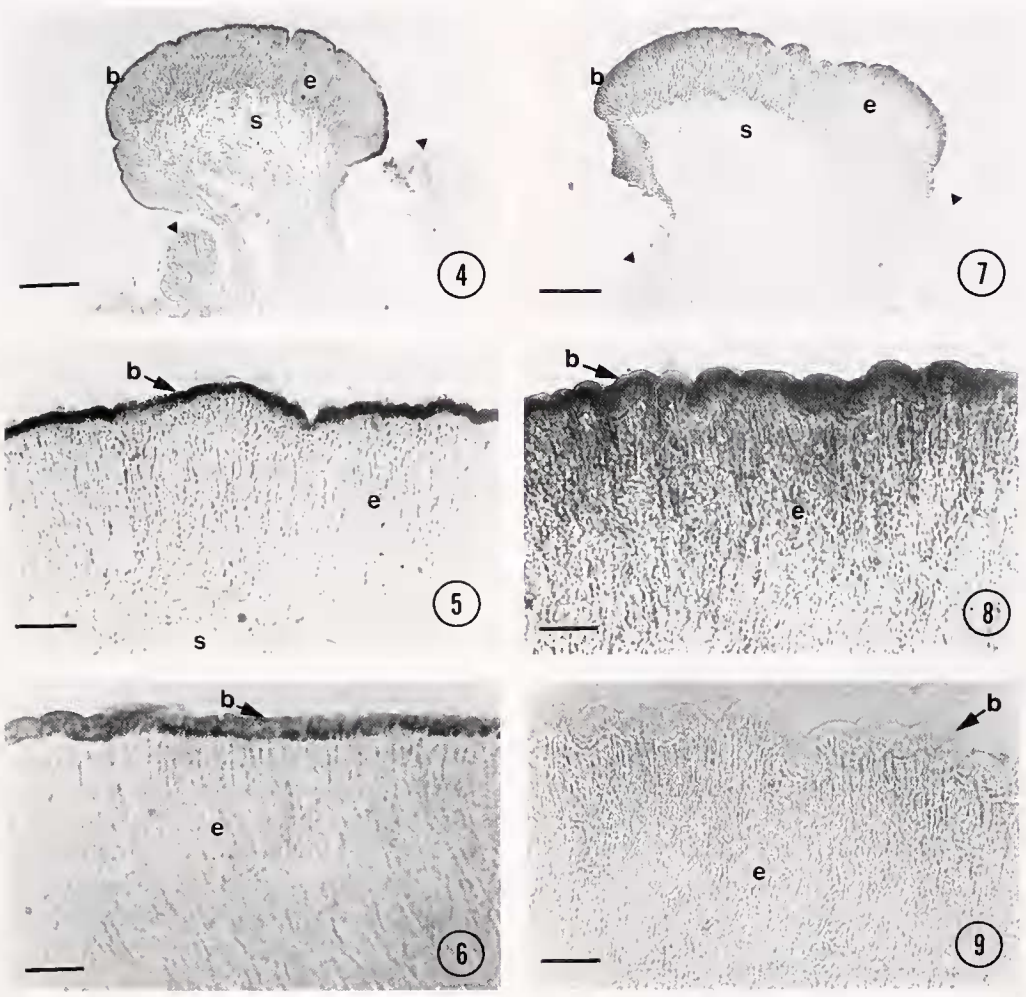

Figures 4–9. Immunohistochemical localization of vacuolar-type ATPase (V-ATPase) in whole accessory boring organ (ABO) of *Nucella lamellosa*.

Figure 4. This section was probed with polyclonal antibody to the V-ATPase d (39-kDa) subunit and alkaline-phosphatase-conjugated secondary antibody. Immunoreactive sites were visualized with BCIP/NBT. Immunostaining is exclusive to the brush border of the ABO (b). Immunostaining is absent in the foot epithelium (arrowheads). e, epithelial cells; s, sinus. Scale bar: 100 μm.

Figure 5. Magnified image of the ABO shown in Figure 4. Note the positive reaction for V-ATPase in the brush border (b). e, epithelium; s, sinus. Scale bar: 75 μm.

Figure 6. This section was probed with the anti-39kDa primary antibody (as above) and HRP-conjugated secondary antibody. Immunoreactive sites were visualized using DAB-H_2O_2. The immunostaining is exclusive to the brush border (b). e, epithelium. Scale bar: 40 μm.

Figure 7. This section was probed with monoclonal antibody to the V-ATPase B (60-kDa) subunit, primary antibody, and alkaline-phosphatase-conjugated secondary antibody. Immunoreactive sites were visualized with BCIP/NBT. Immunostaining is exclusive to the brush border of the ABO (b). Arrowheads, foot epithelium; e, epithelial cells; s, sinus. Scale bar: 100 μm.

Figure 8. Magnified image of the ABO seen in Figure 7. Very intense immunostaining is noted in the brush border (b). e, epithelium. Scale bar: 25 μm.

Figure 9. ABO probed only with alkaline-phosphatase-conjugated secondary antibody and BCIP/NBT. No immunostaining is apparent in the brush border (b). e, epithelium. Scale bar: 25 μm.

tions incubated in anti-B subunit polyclonal antibody showed the same immunostaining pattern. Both the anti-B subunit (Figs. 7 and 8) and anti-A subunit monoclonal antibodies showed positive staining for V-ATPase within the brush border. Control sections incubated without a primary antibody (Fig. 9) exhibited no immunoreaction. Immuno-electron micrographs of a section of an ABO treated with anti-d subunit primary antibody and gold-conjugated secondary antibody showed immunoreactivity (Fig. 10). The reactive sites for the V-ATPase antibody are located in the microvilli of the epithelial cells, as evident by the presence of gold particles in the microvilli. The gold parti-

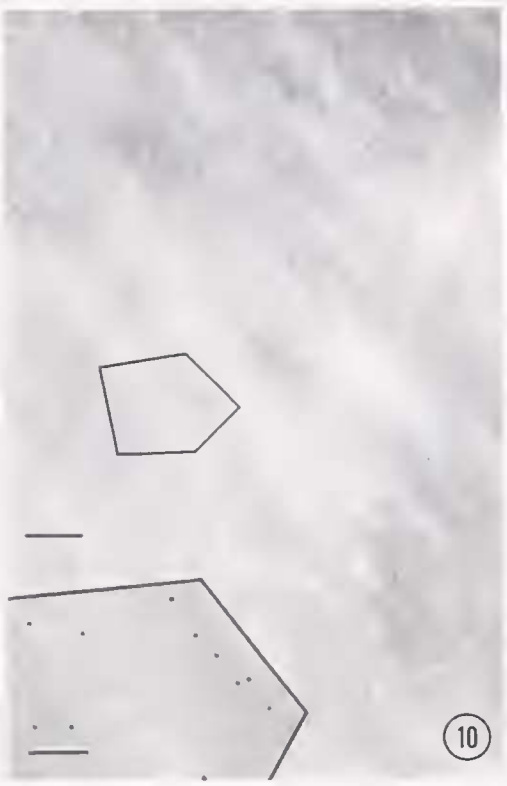

Figure 10. Immuno-electron micrograph of the microvilli (mv) that form the brush border of the accessory boring organ (ABO) of *Nucella lamellosa*. The section was probed with primary antibody to the V-ATPase d (39-kDa) subunit and gold-conjugated secondary antibody. The presence of 10-nm gold particles in the micrograph reveals that the immunoreactive sites for V-ATPases are located in the microvillar membrane. Scale bar: 200 nm. The inset shows the gold particles (outlined in black) that lie close to the plasma membranes of the microvilli. Scale bar: 50 nm.

cles underlie the membranes of the microvilli (inset), since the d subunit closely associates with the transmembrane (V_0) domain in assembled molecules. These results suggest that V-ATPases are present in the plasma membranes of the microvilli of the ABO epithelial cells.

Molecular weight determination

Electropherograms of the 100,000 × *g* membrane resuspension on SDS-polyacrylamide gels (Fig. 11) revealed several peptide bands. Peptides with molecular weights of approximately 70, 60, and 39 kDa (arrowheads) may correspond to subunits A, B, and d, V-ATPase subunits. Other bands corresponding to the remaining V-ATPase subunits (not indicated) are also present. V-ATPase peptides are known to be highly conserved across kingdoms, phyla, genera, and species (Arg[illegible], 1998). Note that in Figure 11, the lower molecular weight standards (17.6 and 7.5 kDa) of the marker lanes run with the dye front (large arrowhead), so that the lower molecular weight peptides are unresolved. The 9% gel was found to be suitable for use in western blotting since markers of 32.6 kDa and higher molecular weights were clearly resolved. The remainder of the bands seen on the gel are presumably peptides of a variety of other membrane molecules (Na^+/K^+-ATPase, ion channel proteins, etc.).

Samples of purified yeast V-ATPase (positive control) and of the 15,000 × *g* gland extract supernatant were applied to PVDF membrane and probed using the polyclonal antibodies and alkaline-phosphatase-conjugated secondary antibodies (Fig. 12). Lane a shows positive immunoreaction to samples of yeast V-ATPase (2-μl samples [top] and 1 μl samples [bottom]) that were probed with the anti-B polyclonal antibody. Lanes b, c, and d were made with samples of the 15,000 × *g* supernatant (15 μg protein [top] and 3 μg protein [bottom]). Lane b and lane c were probed with polyclonal antibodies directed against the B and d V-ATPase subunits respectively. These samples also show positive immunoreactivity. Samples in lane d were incubated without primary antibody and act as negative controls.

Western blots obtained from protein transferred from a 9% SDS-polyacrylamide gel are shown in Figure 13. Markers, indicated on the outside lanes, were also run in the lanes between sections of the membrane incubated in either anti-d (39 kDa) polyclonal antibody (a), anti-B (~60 kDa) polyclonal antibody (b), or without a primary antibody (c). Note that two lanes appear in each section of the blot between the marker lanes. A single nonspecific band occurring slightly below the 70 kDa markers is seen in all the blots. This is probably the result of a protein reacting with the TrueBlue peroxidase substrate. Blot a clearly reveals positive staining with the anti-39-kDa antibody. A single band is observed in each lane somewhat below the 42.8-kDa markers. This band

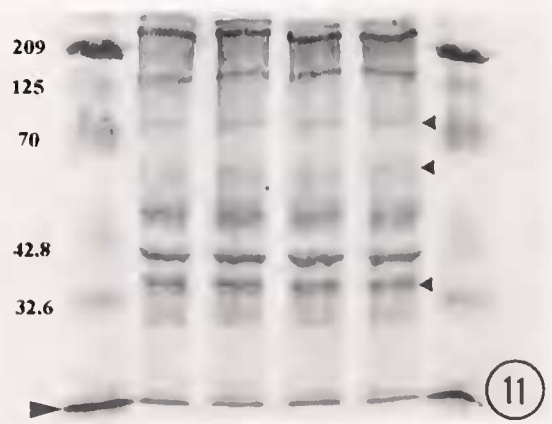

Figure 11. Discontinuous SDS-PAGE (9% gel) of ABO membranes. Molecular weight standards are shown in the outside lanes. The 9% gels were found to be suitable for western blotting, since our antibodies are specific for subunits exceeding 32.6 kDa. The center lanes of the gel show the banding pattern observed in the ABO membrane. Peptides corresponding to the molecular weight of A, B, and d V-ATPase subunits are indicated (arrowheads).

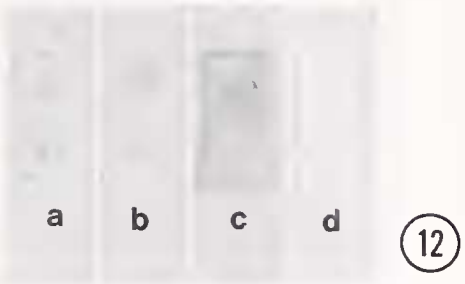

Figure 12. Samples of purified yeast V-ATPase (a: 2 μl, upper; 1 μl lower) and of the 15,000 × *g* supernatant of ABO extract (b, c, d: 15 μg protein, upper; 3 μg protein, lower) were spotted onto PVDF membrane, and probed with primary antibodies and alkaline-phosphatase-conjugated secondary antibodies. Color was developed with BCIP/NBT. a (positive control) and b were probed with the anti-B (~60-kDa) subunit primary antibody, while c was probed with the anti-d (39-kDa) subunit primary antibody. All except d (negative control) show positive staining for V-ATPase.

does not appear in b or c. It appears that the antibody binds to a peptide that has a relative molecular weight corresponding to the subunit against which it was raised. Blot b reveals a positive reaction lying immediately beneath the nonspecific band, at about 60 kDa. It appears that this antibody also recognizes a peptide that corresponds to the subunit against which it was raised. Faint bands occurring in a and b near the 125-kDa marker are possibly due to endogenous peroxidase activity; alternatively, they could reveal peptides with epitopes similar to those recognized by the antibodies. The control blot c shows only the single nonspecific band, indicating that the immunostaining apparent in a and b results from the specific binding of the V-ATPase antibodies to their respective subunits.

ATPase assays

Assays conducted to determine the effect of bafilomycin on the release of Pi reveal that the quantity of Pi detected is significantly lower in samples containing the inhibitor than in the control samples. Three separate homogenates were assayed, and the difference was observed in each case. The results (Table 1) reveal that about 10% of the inorganic phosphate detected in the ATPase assays is liberated by V-ATPase. The remainder of the Pi detected is presumably liberated by other phosphatases present in the homogenates or by the degradation of the Mg^{2+}-ATP substrate during the incubation periods. V-ATPase activity, defined as the average of the mean differences between control and inhibited trials of the three experiments, is 67.0 ± 13.3 (SEM) pmol Pi/(μg protein · min).

Discussion

Muricid snails such as the frilled whelk, *Nucella lamellosa*, normally prey on a variety of invertebrates such as bivalves, gastropods, barnacles, and other small crustaceans that have a protective calcareous external shell. To feed, the snail must usually bore a hole through this shell. Drilling is completed by a chemomechanical process that combines the action of chemical secretions derived from the accessory boring organ (ABO), to soften the shell materials, with the rasping action of the radula on the shell (Carriker, 1981). The secretion is acidic (Carriker and Van Zandt, 1967) and contains degradative enzymes (Webb and Saleuddin, 1977; Carriker and Williams, 1978). Hydrochloric acid is thought to be the inorganic acid secreted by the ABO because the etchings it produces on bivalve shells are similar to those produced by excised ABOs (Carriker *et al.*, 1963; Carriker, 1978, 1981). Webb and Saleuddin (1977) proposed that an acid ATPase pump located on the apical membrane of the ABO is responsible for secreting the acid from the ABO. The presence of V-ATPase pumps in molluscan epithelia has been implied in electrophysiological studies of the outer mantle epithelium in *Unio complanatus* (Hudson, 1993) and in *Anodonta cygnea* (da Costa *et al.*, 1999). Bafilomycin A_1 was seen to collapse the short circuit current across the apical membrane and prevent the extrusion of protons into the mantle cavity. Protons are extruded into this space, where they are buffered by the shell, which is thought to relieve acid loading in the tissues when the clam is closed (Hudson, 1993). Osteoclasts also use V-ATPase pumps located in their ruffled borders (Väänänen *et al.*, 1990) to extrude protons into the extracellular environment. The

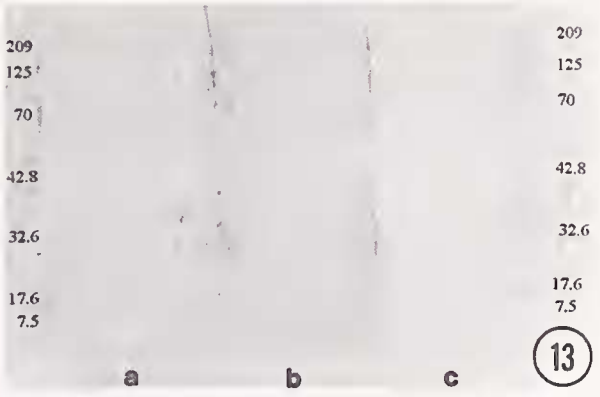

Figure 13. Western blots obtained from membrane preparations. Peptides were transferred onto PVDF membranes from a 9% SDS-PAGE gel. Kaleidoscope markers are shown on each side, and between each blot. The dye front is indicated by the arrowheads. Two lanes appear in each of blots a, b, and c. Blot a was probed with the V-ATPase anti-d (39-kDa) subunit primary antibody and blot b with the anti-B (~60-kDa) subunit primary antibody (polyclonal); c was a negative control. Primary antibodies were detected using a Streptavidin-HRP system, and color was developed using TrueBlue peroxidase substrate. Positive reaction is seen for both V-ATPase subunits, with each antibody binding to its appropriate subunit in the ABO V-ATPase molecule. A single nonspecific band occurring below the 70-kDa marker is seen in a, b, and c. Faint bands seen in and b near the 125-kDa marker are possibly due to endogenous peroxidases or to peptides with epitopes similar to those recognized by the antibodies.

Table 1

ATPase activities in homogenates of accessory boring organ, expressed as nanomoles of inorganic phosphate per microgram of total protein per minute

	Homogenate 1	Homogenate 2	Homogenate 3
Control activity (No inhibitor)	0.4725 ± 0.0026 (5)	1.065 ± 0.0205 (3)	0.6445 ± 0.0060 (4)
Inhibited activity (With bafilomycin)	0.4308 ± 0.0042 (8)	0.993 ± 0.0185 (3)	0.5573 ± 0.0052 (4)
Mean difference (V-ATPase activity)	0.0419***	0.0720*	0.0873**
T	7.20	2.61	11.03
Mean difference/Control mean	0.088 (8.8%)	0.067 (6.7%)	0.136 (13.6%)

The average V-ATPase activity in the three homogenates is 0.067 nmol (67 pmol)/(μg total protein · min) ± 0.0133, or approximately 10% of the average activity in the control assays. Values are mean ± the standard error. The number of experiments is in parentheses. Student's *t* values are indicated (T). Asterisks indicate level of significance: *** $P < 0.0001$; ** $P \leq 0.001$; * $P \leq 0.05$.

osteoclasts anchor to bone, and they extrude protons and chloride ions into bone-resorbing compartments, where the resulting acid dissolves the mineralized component of the bone and activates lysosomal enzymes that break down the bone matrix (Wieczorek *et al.*, 1999). These processes are much like the extrusion of protons from the ABO to dissolve a bivalve shell.

The structure of the ABO in *Nucella lamellosa* was found to conform to that of other muricid gastropods (Carriker *et al.*, 1963; Person *et al.*, 1967; Nylen *et al.*, 1969; Webb and Saleuddin, 1977) and to the analogous regions of the naticid ABO (Bernard and Bagshaw, 1969). The epithelial cells of the ABO have so many mitochondria that they are termed mitochondria-rich (MR) cells. They possess a distinctive brush border that forms a continuum across the ABO surface. These cells communicate *via* gap junctions, and they may respond in unison to chemical or mechanical stimuli. A thin, often indistinct basement membrane separates the MR cells from the underlying hemolymph-filled sinus. This structure presumably allows for efficient transfer of oxygen, nutrients, and metabolites, thus enhancing the aerobic metabolism of the cells (Webb and Saleuddin, 1977), and may also permit elastic stretching of the ABO. Dense granules in the ABO epithelial cells are thought to contain enzymes, such as acid phosphatase, that are secreted from the ABO to dissolve the organic matrix of the substrate being drilled (Webb and Saleuddin, 1977; Carriker and Williams, 1978), thus acting in a fashion similar to lysosomal enzymes secreted by osteoclasts (Wieczorek *et al.*, 1999).

Many of the features described in the epithelial cells of the ABO are common in proton transporting MR cells of other animals, which are known to possess V-ATPases in their plasma membranes (Brown and Breton, 1996). Gap junctions are also known to occur in V-ATPase-containing cells (such as insect follicle cells) in which a coordinated response is required (Harvey *et al.*, 1998). High levels of carbonic anhydrase activity are another feature of these MR cells, and this characteristic is shared by muricid ABOs. The enzyme catalyzes the production of free protons *via* the carbonic acid pathway (Chétail and Fournié, 1969; Webb and Saleuddin, 1977). Elevated cytochrome oxidase, succinic dehydrogenase, and lactate dehydrogenase activities have also been detected in actively drilling muricids (Person *et al.*, 1967), suggesting that the mitochondria are metabolically active during the boring process. Presumably ATP production is linked to increased activity of the V-ATPase proton transporters, which serve to extrude protons from the ABO.

Immunocytochemical staining at the light microscopic level reveals that all four V-ATPase antibodies used in our studies bind to sites within the brush border of the MR cells in the ABO. Immuno-electron microscopy also indicates that the V-ATPase-reactive sites are located in the microvilli of the MR cells. Immunogold particles attached to V-ATPase antibodies are seen to underlie the plasma membrane of the microvilli. This localization occurs because the antibody is directed against the 39-kDa "d" subunit of the enzyme, which closely associates with the transmembrane domain of V-ATPases. These antibodies are known to cross-react with their corresponding subunits in either yeast or bovine samples (pers. comm. from Dr. Morris Manolson, University of Toronto) and in general, V-ATPase antibodies raised against a given species will react with most other V-ATPases (even across kingdoms) because of the homologous nature of their peptide sequences (Russell *et al.*, 1992). Our results are in accord with the localization of V-ATPase in the apical region of MR cells in a variety of animals—for example, in pavement cells in the gills of freshwater fish (Lin *et al.*, 1994; Sullivan *et al.*, 1995); in distal duct cells of the cockroach salivary glands (Just and Walz, 1994); in the midgut, Malpighian tubules, and silk glands of lepidopterans (Schweikel *et al.*, 1989; Pietrantonio and Gill, 1995; Azuma and Ohta, 1998); and in the MR cells of the toad urinary bladder (Brown *et al.*, 1988). V-ATPases have also been localized in the plasma membrane of osteoclasts (Väänänen *et al.*, 1990), for which the

name "single celled epithelia" has been coined (Brown and Breton, 1996).

SDS-PAGE and immunoblotting provided additional immunological evidence to support the identity of V-ATPase pumps. Gel electrophoresis revealed that a membrane preparation of ABO homogenate contains peptides with molecular weights that are similar to those of V-ATPase subunits. Additional bands in the gel reflect the impurity of our sample. Furthermore, dot and western immunoblots of samples derived from ABO homogenates stained positive for V-ATPase. The western blots show that polyclonal antibodies raised against mammalian V-ATPase subunits cross-react to the equivalent peptides of V-ATPases found in the ABO. This suggests that the ABO V-ATPase is homologous to other known V-ATPase species.

Finally, identification of V-ATPase was established pharmacologically using the specific V-ATPase inhibitor bafilomycin A_1 (Bowman *et al.*, 1988). ATPase assays were conducted on the 1000 × *g* supernatant of ABO homogenates obtained from 15–20 animals. Three separate pooled ABO homogenates were produced and assayed for ATPase activity. Each 1000 × *g* supernatant provided sufficient protein to assay a minimum of three control and three inhibited trials. About 10% of the phosphate liberated in the control samples was seen to be derived from V-ATPase. V-ATPase activity ranged from 41.90 to 87.25 pmol Pi/(μg protein · min), with an average of ~67 pmol/(μg protein · min). The disparity in the ATPase activities among the three ABO homogenates can be attributed primarily to variation in the amount of V-ATPase actually present in each homogenate (total protein was determined, so inclusion of excess foot tissue, for example, would lower the V-ATPase content) and to variation in the amount of Pi released through dissociation of endogenous ATP or other phosphorylated substrates during tissue processing and assay procedures. The activity of the ABO V-ATPase is comparable to that reported in other animals: Onken and Putzenlechner (1995) reported V-ATPase activities of 20 and 10 pmol Pi/(μg protein · min) in filtrates from the posterior and anterior gills of *Eriocheir sinensis*, respectively, whereas Al-Fifi *et al.* (1998) found a higher activity of 192.3 pmol Pi/(μg protein · min) in a 600 × *g* supernatant obtained from the homogenates of Malpighian tubules in *Locusta*, and Sallman *et al.* (1986) reported V-ATPase activities of 30.8 pmol Pi/(μg protein · min) and 42.4 pmol Pi/(μg protein · min) in homogenates respectively obtained from the cortex and medulla of human kidneys.

The structural, immunological, and biochemical investigations undertaken in this study provide clear evidence that V-ATPase is present in the ABO of *Nucella lamellosa*, and that this V-ATPase shares structural similarity with other V-ATPase species. On the basis of these findings, we can revise the Webb and Saleuddin (1977) model describing the mechanism of proton transport by a muricid ABO. The revised model (Fig. 14) contains V-ATPase proton pumps in the microvilli of the ABO epithelial (MR) cells. The presumed presence of chloride-bicarbonate antiporters in the basolateral membranes, apical chloride channels, and paracellular chloride transport is consistent with current

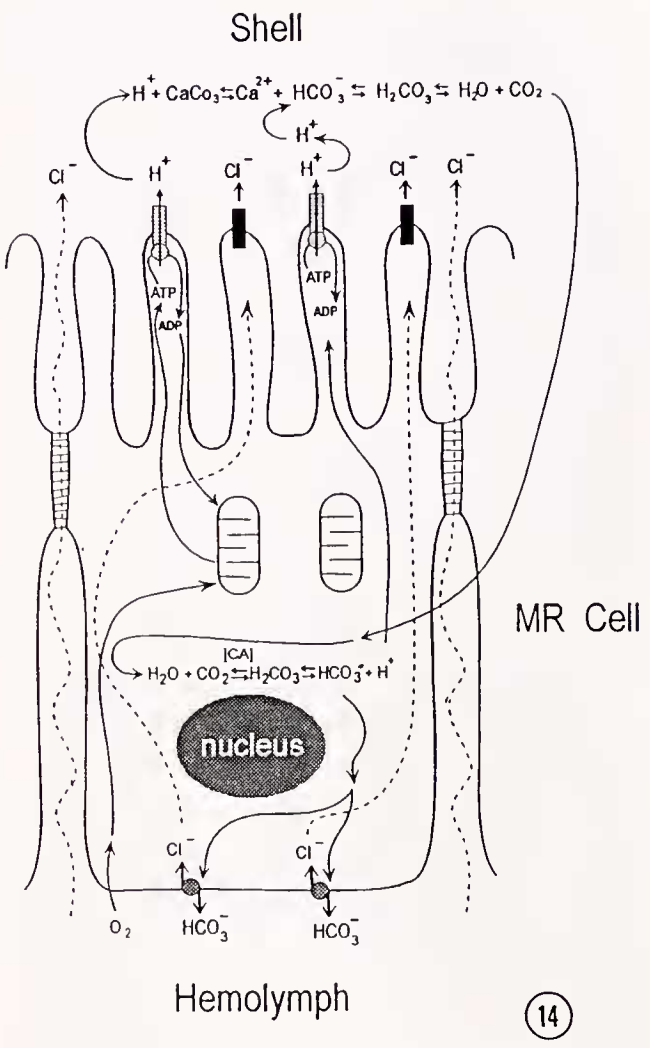

Figure 14. Revised model of the mechanism of proton transport in the muricid accessory boring organ (ABO). Carbonic anhydrase (CA) catalyzes the production of H^+ and HCO_3^- *via* the carbonic acid pathway. Bicarbonate is removed from the mitochondria-rich (MR) epithelial cell *via* basal HCO_3^-/Cl^- antiporters, while protons are extruded from the cell into the bore hole by V-ATPase pumps located in the microvilli. Mitochondria generate ATP to power the extrusion process, generate metabolic CO_2 for the carbonic acid reaction, and provide a reducing environment to stabilize the V-ATPase molecules. Chloride ions exit the cell *via* apical ion channels, and possibly by paracellular routes. The protons and chloride ions (HCl) act to dissolve the mineralized component ($CaCO_3$) of the shell, while degradative enzymes also present in the secretions of the ABO break down the organic matrix. Carbon dioxide liberated from the dissolving shell may diffuse into the cell to enhance the carbonic acid reaction. The presence of HCO_3^-/Cl^- antiporters and, as speculated here, of chloride ion channels is based on comparable studies of mitochondria-rich cells in other animal epithelia.

models describing MR cells in many animal epithelia such as insect Malpighian tubules (Maddrell and O'Donnell, 1992; Beyenbach, 1995; Pannabecker, 1995; Brown and Breton, 1996; Harvey *et al.*, 1998).

V-ATPases actively pump protons from the cytoplasm and extrude them into the bore hole. Chloride is also extruded from the cells *via* ion channels and perhaps paracellularly between the MR cells. Protons combine with the chloride ions in the extracellular space, forming hydrochloric acid. As mentioned, it has been suggested that HCl is the acid in the secretion from muricid and naticid ABOs (Carriker *et al.*, 1963; Carriker, 1978, 1981), and the revised model is consistent with these studies. Bicarbonate is eliminated from the cells into the hemolymph by anion transporters as shown, and chloride is transferred into the cell as a counter ion. Other ion transporters are probably present, but are excluded from this diagram for clarity. The model accounts for all the structural features of the MR cells (as discussed by Webb and Saleuddin, 1977), but it now identifies the proton pump and can account for the presence of HCl in ABO secretions. Moreover, our revised model places the muricid ABO into the group of animal epithelia that use V-ATPase pumps to acidify extracellular environments.

No attempt was made in this study to identify the degradative enzymes in the secretion of the ABO, but our model is not inconsistent with the presence of lysosomal enzymes (such as indicated by Webb and Saleuddin, 1977). Such enzymes could be used to degrade the organic components of shells (*e.g.*, periostracum and shell matrix protein, chitin in crustaceans, or keratinized structures such as elasmobranch egg capsules), in a manner similar to the degradation of bone matrix by lysosomal enzymes secreted by osteoclasts (Wieczorek *et al.*, 1999). Dense granules observed in the MR cells may in fact contain such enzymes. It is well known that one of the major functions of intracellular V-ATPases is the acidification of endosomes such as lysosomes and peroxisomes, particularly in phagocytic cells, which is necessary for the activation of lysosomal enzymes (Grinstein *et al.*, 1992). V-ATPases in the apical membrane of the ABO could serve the same function, acidifying the secretions from the ABO to activate secreted enzymes. Mucus secreted from the goblet cells of the surrounding foot epithelium or from the MR cells of the ABO could serve to protect the ABO from acidic and enzymatic degradation. The localization of V-ATPase pumps in the epithelium of the muricid ABO, reported here, and their presence in the shell-facing mantle epithelia of freshwater bivalves (Hudson, 1993; da Costa *et al.*, 1999) and in the membranes of osteoclasts (Väänänen *et al.*, 1990) suggests that the mechanism for decalcification of calcareous substrates is conserved.

It is interesting to speculate on the method of regulation of the V-ATPases in the ABO. The mechanism could quite simply be the inactivation of the catalytic domains or their dissociation from the proton-transporting domains when the ABO is flaccid, and the reactivation/reassociation of the V-ATPases in engorged organs. In the engorged state, hemolymph filling the sinus of the ABO would aerate the MR cells, enabling enhanced aerobic metabolism in the mitochondria. In addition to producing ATP as the energy source, this activity could produce a reducing environment in the apical region of the cells, stabilizing the V-ATPase pumps (Merzendorfer *et al.*, 1997). In the flaccid state, blood supply is shut off to the ABO, inhibiting aerobic metabolism and leading to the oxidation and inactivation of the V-ATPases. It is also possible that factors acting as hormones enter the ABO *via* the hemolymph and pass through the thin basement membrane of the MR cells to act on the V-ATPases. Their effects may be direct, or they may act through mediators such as the 35-kDa V-ATPase cytosolic activator peptide in bovine kidneys (Zhang *et al.*, 1992).

Acknowledgments

This study was supported by a grant from NSERC, Canada to ASMS. We thank Dr. Sergio Grinstein and Dr. Morris Manolson of the University of Toronto for their gifts of antibodies, Dr. Michael O'Donnell of McMaster University for his insights into invertebrate V-ATPases, and Drs. Hamid Khan and Spencer Mukai of York University, for their technical assistance. Thanks also to Dr. Barry G. Loughton for editing the manuscript.

Literature Cited

Al-Fili, Z. I. A., S. L. Marshall, D. Hyde, J. H. Anstee, and K. Bowler. 1998. Characterization of ATPases of apical membrane fractions from *Locusta migratoria* Malpighian tubules. *Insect Biochem. Mol. Biol.* **28:** 201–211.

Atkinson, A., A. D. Gatenby, and A. G. Lowe. 1973. The determination of inorganic orthophosphate in biological systems. *Biochim. Biophys. Acta* **320:** 195–204.

Azuma, K., and Y. Ohta. 1998. Changes in H^+-transporting vacuolar-type ATPase in the anterior silk gland of *Bombyx mori* during metamorphosis. *J. Exp. Biol.* **201:** 479–486.

Bernard, F. R., and J. W. Bagshaw. 1969. Histology and fine structure of the accessory boring organ of *Polinices lewisi* (Gastropoda, Prosobranchia). *J. Fish. Res. Board Can.* **26:** 1451–1457.

Beyenbach, K. W. 1995. Mechanism and regulation of electrolyte transport in Malpighian tubules. *J. Insect Physiol.* **41:** 197–207.

Bowman, E. J., A. Siebers, and K. Altendorf. 1988. Bafilomycins: a class of inhibitors of membrane ATPases from microorganisms, animal cells, and plant cells. *Proc. Natl. Acad. Sci. USA* **85:** 7972–7976.

Bradford, M. 1976. A rapid and sensitive method for the quantitation of microgram quantities of protein utilizing the principle of protein-dye binding. *Anal. Biochem.* **72:** 248–254.

Brown, D., and S. Breton. 1996. Mitochondria-rich proton-secreting epithelial cells. *J. Exp. Biol.* **199:** 2345–2358.

Brown, D., S. Hirsch, and S. Gluck. 1988. Localization of a proton-pumping ATPase in rat kidney. *J. Clin. Invest.* **82:** 2114–2126.

Brown, D., P. J. S. Smith, and S. Breton. 1997. Role of V-ATPase-rich cells in acidification of the male reproductive tract. *J. Exp. Biol.* **200:** 257–262.

Carriker, M. R. 1978. Ultrastructural analysis of dissolution of the shell

of the bivalve *Mytilus edulis* by the accessory boring organ of the gastropod *Urosalpinx cinerea*. *Mar. Biol.* **48:** 105–134.

Carriker, M. R. 1981. Shell penetration and feeding by naticacean and muricacean predatory gastropods: a synthesis. *Malacologia* **20:** 403–422.

Carriker, M. R., and D. Van Zandt. 1967. Gastropod *Urosalpinx*: pH of accessory boring organ while boring. *Science* **158:** 920–922.

Carriker, M. R., and L. G. Williams. 1978. The chemical mechanism of shell dissolution by predatory boring gastropods: a review and an hypothesis. *Malacologia* **17:** 143–156.

Carriker, M. R., D. B. Scott, and G. N. Martin. 1963. Demineralization mechanism of boring gastropods. Pp. 55–89 in *Mechanisms of Hard Tissue Destruction*, R. F. Sognannaes, ed. American Association for the Advancement of Science, Washington, DC.

Chétail, M., and J. Fornié. 1969. Shell-boring mechanism of the gastropod *Purpura (Thais) lapillus*: a physiological demonstration of the role of carbonic anhydrase in the dissolution of $CaCO_3$. *Am. Zool.* **9:** 983–990.

Collins, T. M., K. Frazer, A. R. Palmer, G. J. Vermeij, and M. R. Brown. 1996. Evolutionary history of northern hemisphere *Nucella* (Gastropoda, Muricidae): Molecular, morphological, ecological, and paleontological evidence. *Evolution* **50:** 2287–2304.

da Costa, A. R., P. F. Oliveira, C. Barrias, and H. G. Ferreira. 1999. Identification of a V-type proton pump in the outer mantle epithelium of *Anodonta cygnea*. *Comp. Biochem. Physiol.* **123:** 337–342.

Ehrenfeld, J., and U. Klein. 1997. The key role of the H^+ V-ATPases in acid-base balance and Na^+ transport processes in frog skin. *J. Exp. Biol.* **200:** 247–256.

Finbow, M. E., and M. A. Harrison. 1997. The vacuolar H^+-ATPase: a universal proton pump of eukaryotes. *Biochem. J.* **324:** 697–712.

Forgac, M. 1998. Structure, function and regulation of the vacuolar (H^+)-ATPases. *FEBS Lett.* **440:** 258–263.

Fretter, V., and A. Graham. 1962. Chapter 10: Feeding. Pp. 240–262 in *British Prosobranch Molluscs. Their Functional Anatomy and Ecology*. The Ray Society. London.

Grinstein, S., A. Nanda, G. Lukacs, and O. Rotstein. 1992. V-ATPases in phagocytic cells. *J. Exp. Biol.* **172:** 179–192.

Harvey, W. R., S. H. P. Maddrell, W. H. Telfer, and H. Wieczorek. 1998. H^+ V-ATPases energize animal plasma membranes for secretion and absorption of ions and fluids. *Am. Zool.* **38:** 426–441.

Hudson, R. L. 1993. Bafilomycin-sensitive acid secretion by mantle epithelium of the freshwater clam, *Unio complanatus*. *Am. J. Physiol.* **264:** R946–R951.

Humason, G. L. 1967. *Animal Tissue Techniques*. 2nd ed. W. H. Freeman, San Francisco. Pp. 16, 165.

Just, F., and B. Walz. 1994. Immunocytochemical localization of Na^+/K^+ ATPase and V-H^+-ATPase in the salivary glands of the cockroach, *Periplaneta americana*. *Cell Tissue Res.* **278:** 161–170.

Laemmli, U. K. 1970. Cleavage of structural proteins during the assembly of the head of bacteriophage T4. *Nature* **227:** 680–685.

Lin, H., D. C. Pfeiffer, A. W. Vogl, J. Pan, and D. J. Randall. 1994. Immunolocalization of H^+-ATPase in the gill epithelia of rainbow trout. *J. Exp. Biol.* **195:** 169–183.

Lubansky, H. J., and A. L. Arruda. 1985. Plasma membrane proton-ATPase of a turtle bladder epithelial cell line. *J. Biol. Chem.* **260:** 4035–4040.

Maddrell, S. H. P., and M. J. O'Donnell. 1992. Insect Malpighian tubules: V-ATPase action in ion and fluid transport. *J. Exp. Biol.* **172:** 417–429.

McLean, I. W., and P. K. Nakane. 1974. Periodate-lysine-paraformaldehyde: a new fixative for immunoelectron microscopy. *J. Histochem. Cytochem.* **22:** 1077–1083.

Merzendorfer, H., R. Gräf, M. Huss, W. R. Harvey, and H. Wieczorek. 1997. Regulation of proton-translocating V-ATPases. *J. Exp. Biol.* **200:** 225–235.

Nelson, N., and W. R. Harvey. 1999. Vacuolar and plasma membrane proton-adenosine-triphosphatases. *Physiol. Rev.* **79:** 361–385.

Nordström, T., L. D. Shrode, O. D. Rotstein, R. Romanek, T. Goto, J. N. M. Heersche, M. F. Manolson, G. F. Brisseau, and S. Grinstein. 1997. Chronic extracellular acidosis induces plasmalemmal vacuolar type H^+ ATPase activity in osteoclasts. *J. Biol. Chem.* **272:** 6354–6360.

Nylen, M. U., D. V. Provenza, and M. R. Carriker. 1969. Fine structure of the accessory boring organ of the gastropod *Urosalpinx*. *Am. Zool.* **9:** 935–965.

Onken, H., and M. Putzenlechner. 1995. A V-ATPase drives active, electrogenic and Na^+-independent Cl^- absorption across the gills of *Eriocheir sinensis*. *J. Exp. Biol.* **198:** 767–774.

Pannabecker, T. 1995. Physiology of the Malpighian tubule. *Annu. Rev. Entomol.* **40:** 493–510.

Pantin, C. F. A. 1964. Narcotization. Pp. 5–7 in *Notes On Microscopical Technique for Zoologists*. Cambridge University Press, London.

Person, P., A. Smarsh, S. J. Lipson, and M. R. Carriker. 1967. Enzymes of the accessory boring organ of the muricid gastropod *Urosalpinx cinerea follyensis*. I. Aerobic and related oxidative systems. *Biol. Bull.* **133:** 401–410.

Pietrantonio, P. V., and S. S. Gill. 1995. Immunolocalization of the 17 kDa vacuolar H^+-ATPase subunit c in *Heliothis virescens* midgut and Malpighian tubules with an anti-peptide antibody. *J. Exp. Biol.* **198:** 2609–2618.

Rautiala, T. J., A. M. P. Koskinen, and H. K. Väänänen. 1993. Purification of vacuolar ATPase with bafilomycin C_1 affinity chromatography. *Biochem. Biophys. Res. Commun.* **194:** 50–56.

Russell, V. E. W., U. Klein, M. Reuveni, D. D. Spaeth, M. G. Wolfersberger, and W. R. Harvey. 1992. Antibodies to mammalian and plant V-ATPases cross react with the V-ATPase of insect cation-transporting plasma membranes. *J. Exp. Biol.* **166:** 131–143.

Sallman, A. L., H. J. Lubansky, Z. Talor, and J. A. L. Arruda. 1986. Plasma membrane proton ATPase from human kidney. *Eur. J. Biochem.* **157:** 547–551.

Schweikl, H., U. Klein, M. Schindlbeck, and H. Wieczorek. 1989. A vacuolar-type ATPase, partially purified from potassium transporting plasma membranes of tobacco hornworm midgut. *J. Biol. Chem.* **264:** 11136–11142.

Sheng, S., and S. M. Schuster. 1992. Simple modifications of a protein immunoblotting protocol to reduce nonspecific background. *Biol. Techniques* **13:** 704–708.

Sullivan, G. V., J. N. Fryer, and S. F. Perry. 1995. Immunolocalization of proton pumps (H^+-ATPase) in pavement cells of rainbow trout gill. *J. Exp. Biol.* **198:** 2619–2629.

Väänänen, H. K., E.-K. Karhukorpi, K. Sundquist, B. Wallmark, I. Roininen, T. Hentunen, U. Tuukkanen, and P. Lakkakorpi. 1990. Evidence for the presence of a proton pump of the vaculolar H^+-ATPase type in the ruffled border of osteoclasts. *J. Cell Biol.* **111:** 1305–1311.

Webb, R. S., and A. S. M. Saleuddin. 1977. Role of enzymes in the mechanism of shell penetration by the muricid gastropod, *Thais lapillus* (L.). *Can. J. Zool.* **55:** 1846–1857.

West, L. 1986. Intertidal variation in prey selection by the snail *Nucella (=Thais) emarginata*. *Ecology* **67:** 798–809.

West, L. 1988. Prey selection by the tropical snail *Thais melones*: a study of interindividual variation. *Ecology* **69:** 1839–1854.

Wieczorek, H., D. Brown, S. Grinstein, J. Ehrenfeld, and W. R. Harvey. 1999. Animal plasma membrane energization by proton-motive V-ATPases. *BioEssays* **21:** 637–648.

Zhang, K., Z. Q. Wang, and S. Gluck. 1992. Identification and partial purification of a cytosolic activator of H^+-ATPases from mammalian kidney. *J. Biol. Chem.* **267:** 9701–9705.